CHAPTER 2 LITERATURE SURVEY

Literature survey of any research filed or subject is must required, before contributing in the research of that field. The literature review gives a detailed study of existing published material for clear understanding of that area. Therefore, this chapter presents a detailed literature survey of the area taken (i.e., OFDM). The study in this chapter highlights different problems or issues of OFDM system like high PAPR, synchronization, and Inter-Carrier-Interference (ICI). This review also summarizes the methods available in the literature to overcome these problems.

2.1 INTRODUCTION

The demand for broadband wireless communications is growing with an extremely rapid pace. These systems are required to be operating in an environment which is characterized by high carrier frequency, data transmission rate and mobility; altogether such an environment can be modeled by a frequency selective fast time varying fading channel. It has been studied and established, that the multicarrier data transmission techniques such as MC-CDMA and OFDM are best suited for such channels [**11, 39, 52, 69, 102, 106, 113, 120, 124**].

The OFDM is a special case of multicarrier modulation in which serial stream of data is divided in parallel and then modulated by orthogonal sub-carriers with partial overlapping frequency bands. The OFDM symbols have relatively long time duration as compared to single carrier modulation with a narrow bandwidth. This increases the robustness against multipath deteriorations and results in less complex equalizers which helps in performing the channel equalization easily in the frequency domain through a bank of one-tap multipliers **[45, 52 and 102]**. The main advantage of using OFDM system is to increase the robustness against frequency selective fading or narrowband interference. Due to its advantageous features (like high data transmission rate, high bandwidth efficiency, robustness against multi-path fading and less complex equalizer), the OFDM has also been adopted as a major data transmission technique by many wireless communication standards [**28, 32, 33, 34, 46-51**]. Although, the studies and system based on the concept of orthogonal frequency transmission have been publishing since 1958 [**18, 31, 37, 82, 89, 90, 98, 103, 104**], the most of the application using current form of OFDM was develop during 1980s and 90s [**10, 14, 29, 30, 44, 59, 62, 70, 80, 93, 112, 132**].

In spite of several advantageous features, the OFDM systems have two major concerns i.e. high PAPR of transmitted signal and synchronization (timing and frequency) at the receiver. The effects of all these issues are appearing in the form of inter-carrier and inter-symbol interference. Therefore, for overall improvement in the performance of OFDM system, it is required to handle all these issues separately. Lot of work has been reported in literature regarding these problems. Most of the work published in the late 1990s and 2000s was related to these problems, the focus of work was on the analysis and solution of these problems. This literature survey provides a brief review of all the published material regarding the analysis and solution of these problems of OFDM system. The next section elaborates these issues.

2.2 OFDM SYSTEM MODEL

The discrete time baseband OFDM system model with N subcarriers is shown in Figure 2.2.1. It consists of transmitter, channel and receiver blocks which are described below.

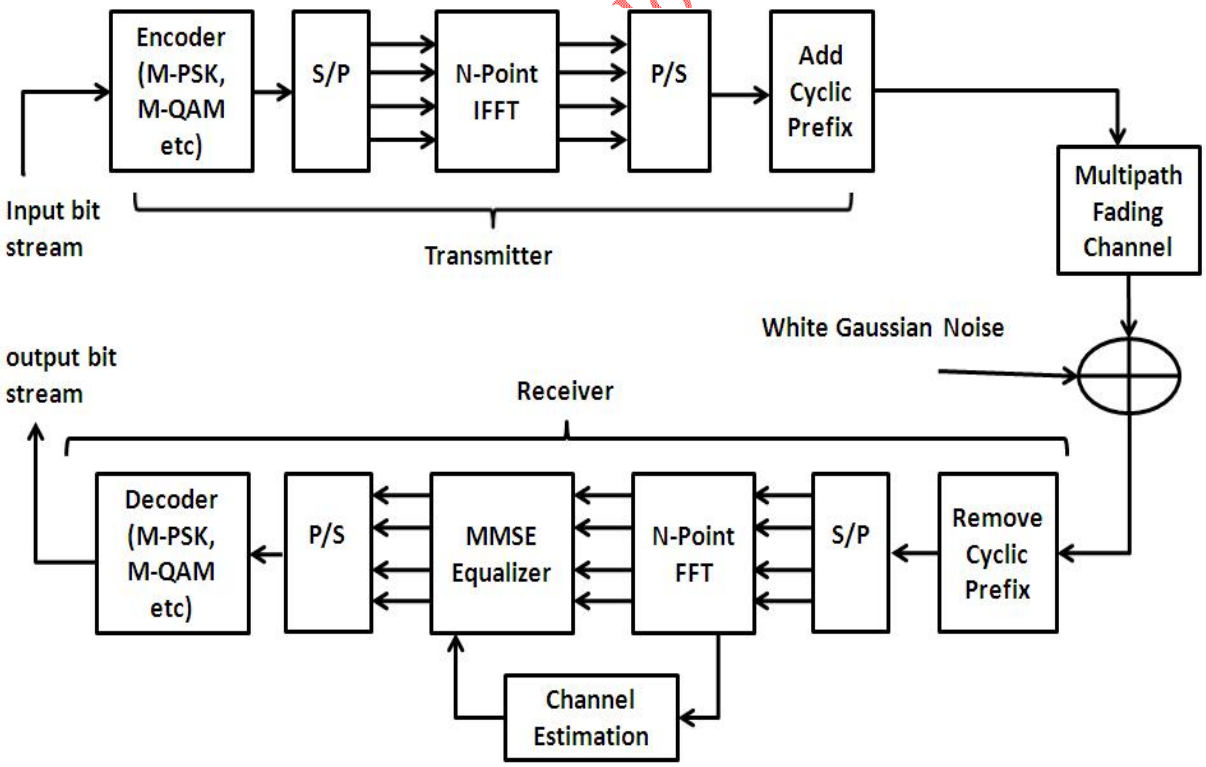

Figure-2.2.1: Baseband OFDM system model

2.2.1 OFDM Signal Generation

At the transmitter, a block of $'N'$ complex data symbols $\{X(k),\ for\ k = 0, 1, 2, \dots, N-1\}$ are first converted from serial to parallel. The complex data symbols are obtained by encoding $log_2(M)$ input bits using modulation techniques like M-PSK, M-QAM, etc. These complex parallel data symbols are then modulated by a group of orthogonal sub-carriers, which satisfy the following condition of orthogonality [**102**]–

$$\frac{1}{T_u}\int_0^{T_u} e^{j2\pi f_k t}\ e^{j2\pi f_m t}\ dt\ =\ \begin{cases}1, & k = m\\ 0, & k \neq m\end{cases}, \qquad \textbf{(2.2.1.1)}$$

where, $f_k = k/T_u$, $for\ k = 0, 1, 2, \dots, N-1$ and $1/T_u$ is the minimum sub-carrier spacing required. The baseband OFDM signal transmitted during i^{th} block can be written as **[102]**–

$$x(i,t) = \frac{1}{N}\sum_{k=0}^{N-1} X(i,k)\ e^{j\,2\pi f_k t},\quad for\ \ 0 \le t \le T_u \qquad \textbf{(2.2.1.2)}$$

where, $T_u(= NT_s)$ is the useful duration of one OFDM symbol, T_s is the sampling interval, $f_k\ (= k/T_u)$ is the sub-carrier frequency of the k^{th} sub-carrier, $X(i,k)$ is the complex data symbol of i^{th} block, modulated on k^{th} sub-carrier, N is the total number of sub-carriers. It is assume that the complex data symbols are uncorrelated. That is –

$$E[X(i,k)\ X^*(i,m)] = \begin{cases}1, & k = m\\ 0, & k \neq m\end{cases}, \qquad \textbf{(2.2.1.3)}$$

where, $X^*(i,m)$ represents the complex conjugate of $X(i,m)$. The discrete version of the baseband OFDM signal $x(i,n)$ can be expressed as –

$$x(i,n) = \frac{1}{N}\sum_{k=0}^{N-1} X(i,k)\ e^{j\,2\pi k n\,/\,N},\qquad for\ \ n = 0, 1, \dots, N-1 \qquad \textbf{(2.2.1.4)}$$

It is clearly visible from (2.2.1.4) that the transmitted signal is the inverse discrete Fourier transform (IDFT) of the complex input data symbols $X(i,k)$ and hence it can be easily and efficiently generated using inverse fast Fourier transform (IFFT) as shown in Figure- 2.2.1. Similarly, the fast Fourier transform (FFT) can be used at the receiver side for demodulation.

2.2.2 Cyclic Prefix or Guard Band Insertion

A guard band interval is usually inserted between successive OFDM symbols to avoid the inter-symbol interference (ISI) caused due to the delay spread of multipath channel. If a guard band interval with no signal transmission is inserted then the ISI can be eliminated almost completely, but a sudden change of waveform contains higher spectral components, so they result in ICI. Therefore the guard interval insertion technique with cyclic prefix (CP) is generally used to avoid ICI.

This scheme was first introduced by Peled and Ruiz in 1980 **[10]**. A technique of cyclic extension (CE) (more commonly referred to today as CP) was suggested as a solution of maintaining the orthogonality when signal is passed through multipath fading channel. In this method, the OFDM symbol is cyclically extended in the guard time [**10**]. The CP insertion is shown in Figure 2.2.2.1.

This technique effectively converts the linear convolutive channel to simulate a channel performing cyclic convolution ensuring orthogonality over a time dispersive channel and eliminating ISI completely between subcarriers as long as the CE remains longer than the impulse response of the channel. However, the CE induces a loss in effective data rates, but the zero ICI generally compensates for the reduction.

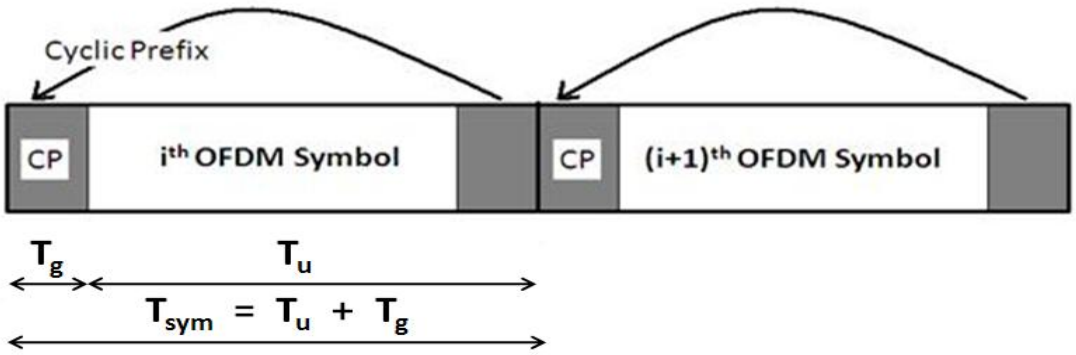

Figure-2.2.2.1: OFDM symbol with cyclic prefix

Due to CP insertion; the transmitted signal is extended to $T_{sym} = T_u + T_g$ and can be expressed as –

$$\tilde{x}(i,t) = \sum_{k=0}^{N-1} X(i,k)\, e^{j\,2\,\pi\, f_k\, t}, \quad for\ -T_g \leq t \leq T_u$$

where, $\tilde{x}(i,t) = x(i,\ t + T_u), \quad for\ -T_g \leq t \leq 0$ **(2.2.2.1)**

The discrete version of the baseband OFDM signal with CP can be expressed as –

$$x(i,n) = \begin{cases} x(i,n+N), & for\ n = 0,1,\ldots,G-1. \\ \dfrac{1}{N}\displaystyle\sum_{k=0}^{N-1} X(i,k)\, e^{j\,2\,\pi\, k\,(n-G)\,/\,N}, & for\ n = G, G+1,\ldots,G+N-1. \end{cases}$$

(2.2.2.2)

where, N is total number of sub-carriers and G is total number of CP samples appended in an OFDM symbol during i^{th} block transmission.

The length of guard interval or CP plays an important role in the performance of OFDM system. If the length of the CP is set shorter than the maximum delay of a multipath channel, the tail part of an OFDM symbol affects the head part of the next symbol, resulting in the ISI. On the other hand a long CP interval increases the overhead of the system. Even if the length of CP is set longer than the maximum delay of the multipath channel, ISI and/or ICI may occur depending on the timing of the FFT window start point (which is usually decided by timing estimation algorithms employed in the system). More specifically, if the FFT window start point is earlier than the lagged end of the previous symbol, ISI occurs; if it is later than the beginning of a symbol, not only ISI (caused by the next symbol), but ICI also occurs [**10, 113**].

2.2.3 Channel Model

The OFDM system is generally used in wireless environment therefore the multipath fading channel has been considered in the present study. The tap-delay line model with L-path is considered for frequency selective fading channel. The impulse response $h(\tau, t)$ for this channel, as given in [**55, 77 and 127**], is –

$$h(\tau,t) = \sum_{l=0}^{L-1} h_l(t)\, \delta(t - \tau_l)\ ,$$

(2.2.3.1)

where, $h_l(t)$ is a tap coefficient and τ_l is a propagation delay of the l^{th} path, respectively. The tap coefficients $h_l(t)$ $(l = 1, 2, 3, \cdots, L)$ are modeled as zero mean complex Gaussian random variables having variances σ_l^2 with $\sigma_1^2 + \sigma_2^2 + \sigma_3^2 + \cdots + \sigma_L^2 = 1$.

2.2.4 Receiver Model

At the receiver, after finding the start of frame (using timing estimation and correction), the CP is removed and the sample of OFDM symbol is converted from serial to parallel. Then, these parallel samples are applied for FFT operation. After FFT, the channel equalization has been done. These equalized data is applied for decoding process to recover information symbol. After considering the effect of multipath fading channel $h(\tau, t)$, the i^{th} received signal $r(i, t)$ can be expressed as –

$$r(i,t) = \sum_{l=0}^{L-1} h_l(\tau)\, \tilde{x}(i, t - \tau_l) + w(i,t), \qquad \textbf{(2.2.4.1)}$$

where, $w(i, t)$ represents the additive white Gaussian noise (AWGN) at the receiver with two sided power spectral density of $N_o/2$. If the length of CP is more than the maximum delay spread of multipath channel and if there is no timing and frequency offsets or the timing and frequency offsets are correctly estimated and corrected then the OFDM symbol can be correctly recovered from the received signal. By considering above condition and after removing the CP, the received signal is given to the FFT block. The output of FFT, $\hat{X}(i, k)$, can be expressed as –

$$\hat{X}(i,k) = H(k)\, X(i,k) + W(i,k), \qquad for\ k = 0, 1, \ldots, N-1 \qquad \textbf{(2.2.4.2)}$$

where, $H(k)$ denotes the frequency response of the multipath fading channel at the k^{th} sub-channel and $W(k)$ is the AWGN component in frequency domain. The frequency response of channel is defined as –

$$H(k) = \sum_{l=0}^{L-1} h_l(\tau)\, e^{-j\, 2\, \pi\, k\, \tau_l\, /\, N} \qquad \textbf{(2.2.4.3)}$$

It is clearly visible in (2.2.4.2) that the complex data symbol $X(i,k)$ can be correctly recovered by a single complex multiplication of factor $G(k)$, where $G(k)$ is the gain of single tap frequency domain equalizer (FEQ) and is defined as –

$$G(k) = 1 / H(k) \qquad \textbf{(2.2.4.4)}$$

The gain $G(k)$ of equalizer can be determine by using any channel estimation techniques which is available in the literature and is given as-

2.2.5 Channel Estimation

The channel estimation techniques for OFDM based systems can be grouped mainly into blind and non-blind categories [**72, 76, 109, 117, 137, and 138**]. The blind channel estimation methods use the statistical behavior of the received signals and require a large amount of data. Hence, they suffer severe performance degradation in fast fading channels. On the other hand, in the non blind channel estimation methods, information of previous channel estimates or some portion of the transmitted signal are available to the receiver to be used for the channel estimation [**76**]. The non-blind channel estimation can be studied under two main groups: Data Aided Channel Estimation (DACE) and Decision Directed Channel Estimation (DDCE).

2.2.5.1 DACE

In data aided channel estimation, a complete OFDM symbol or a portion of a symbol, which is known at the receiver (pilot information), is transmitted so that the receiver can easily estimate the radio channel by demodulating the received samples. There are basically two main issues which affect the performance of any data aided channel estimators. The first issue is the design and arrangement of pilot information [**109**]. The second issue is the design of an estimator or an interpolator with both low complexity and good channel tracking ability [**138**]. These two issues are interconnected. The two basic 1D data aided channel estimations are block-type pilot channel estimation and comb-type pilot channel estimation, in which the pilots are inserted in the frequency direction and in the time direction, respectively.

For slow fading channel and for burst type data transmission schemes, where the channel is assumed to be constant over the burst, the block- type pilot arrangement is usually considered. In this case the pilot tones are assigned to all subcarriers of a particular OFDM symbol so that an OFDM training symbol can be obtained. Due to this reason it is also called as training symbol type. The training symbols are then inserted at the beginning of the bursts to estimate the channel frequency response (e.g. WLAN and Wi-MAX systems). The estimations for the block-type pilot arrangement can be based on least square (LS), minimum mean-square error (MMSE), and modified MMSE algorithms. For the fast fading channel the training symbol should be inserted periodically or the DDCE method should be used so that the channel estimates are updated.

When channel varies between consecutive OFDM symbols (fast fading channel), the comb-type pilot arrangement is generally preferred. In comb-type channel estimation, the known information is being sent with data. This known information which is multiplexed with data to form an OFDM symbol is also called as pilot tones; therefore sometimes comb-type is also called as pilot-aided channel estimation. For the same percentage of overhead, the comb-pilot-aided estimation outperforms the training block-aided methods, particularly for a system with high mobility [137]. The estimation accuracy can be improved by increasing the pilot density. However, this introduces overhead and reduces the spectral efficiency. The estimations for the comb-type pilot arrangement includes the LS estimator with 1D interpolation, the maximum likelihood (ML) estimator, and the parametric channel modeling-based (PCMB) estimator.

2.2.5.2 DDCE

For fast fading channel, where the channel varies between consecutive OFDM symbols, the DDCE methods are generally used for channel estimation. In the DDCE methods, to decode the current OFDM symbol the channel estimates for a previous OFDM symbol are used. The channel corresponding to the current symbol is then estimated by using the newly estimated symbol information. Since an outdated channel is used in the decoding process, these estimates are less reliable as the channel can vary drastically from symbol to symbol [72, 117]. Hence, additional information is usually incorporated in DDCE such as periodically sent training symbols. Channel coding, interleaving, and iterative type approaches are also commonly applied to boost the performance of DDCE techniques.

Although DDCE is simple, it inherently introduces two basic problems: the use of outdated channel estimates, and the assumption of correct data detection. The use of outdated channel estimates

does not pose a serious issue when the channel is varying very slowly. However, when the channel varies fast then the outdated channel estimates for the previous OFDM symbol are no longer valid for the use of the data detection in the current OFDM symbol **[72, 117].** In this case, the data detection would be incorrect, so are the newly estimated channel coefficients. Hence, the error in the channel estimation and data detection build up to make the system performance unacceptable. As a quick solution to overcome the problem related to the outdated channel estimates, the training symbols can be sent more often.

2.3 PEAK TO AVERAGE POWER RATIO (PAPR)

High PAPR of transmitted signals is one of the major issues of the OFDM system. The PAPR of any signal is defined as the ratio between the maximum instantaneous power of signal and its average power. A large dynamic range of input data symbols is the main cause of getting high PAPR. An OFDM signal consists of N independent data symbols modulated on N orthogonal subcarriers, and when these N signals are added with the same phase, high peak amplitude is observed. The value of this peak may be N times of the average amplitude.

Most of the wireless communication systems employed high power amplifier (HPA) at the output of transmitter to obtain sufficient transmits power for large area coverage. For achieving maximum power efficiency, the HPA is usually operated at or near the saturation region. When high peak power signal pass through such HPA, peaks are clipped non-linearly and inter-modulation distortion are induced at the output. This additional interference leads to an increase in BER. This distortion can be minimized, if amplifier operates in linear region. However, this linear amplifier has poor efficiency and is so expensive. Also it reduces the coverage area. Hence, a better solution is to reduce the PAPR before applying the signal to HPA. **[114, 122]**

OFDM system also utilized digital-to-analog converters (DAC) and analog-to-digital converters (ADC) in its signal processing loop. To support high PAPR, a high precision DAC and ADC are required, which is very expensive for a given sampling rate of the system. Whereas, a low-precision DAC and ADC would be cheaper, but its quantization noise will be significant, and as a result it reduces the SNR when the dynamic range of DAC and ADC increases to support high PAPR. Thus, the PAPR reduction is essential for an OFDM system for achieving better power efficiency, large area coverage and low BER. Different types of PAPR reduction techniques are discussed in following section.

2.3.1 PAPR Reduction Techniques

Several PAPR reduction techniques are available in the literature. These methods are basically divided in four categories:

(I) Signal Distortion.
(II) Coding Methods,
(III) Probabilistic (Scrambling) Techniques
(IV) Pre-distortion Methods.

Every method has some drawbacks and merits. There is always a trade-off between PAPR reduction and some other factors like bandwidth, computational complexity, average power etc. An ideal PAPR reduction technique should have following characteristics **[122, 139]**:

(a) High capability of PAPR reduction with few harmful side effects such as in-band distortion and out-of-band radiation.
(b) Low implementation complexity: Due to high implementation and computational complexity the delay in transmission increases which reduces data rate.
(c) Low average power: any increase in average power requires a larger linear operation region in HPA and thus resulting in the degradation of BER performance.
(d) No bandwidth expansion: The bandwidth is a costlier resource for any wireless communication systems. Therefore, it is required to reduce PAPR without increasing bandwidth of transmitted signal. The bandwidth expansion directly results in the data code rate loss due to side information. Therefore, the loss in bandwidth due to side information should be avoided or at least be kept minimal.
(e) No BER performance degradation: The PAPR should be reduce but not at the cost of BER reduction. The BER performance should be same as that of the original OFDM system.
(f) Without additional power needed: Any increases in power requirement reduce the efficiency of system, and power is an important resource for any wireless communication system. Therefore, it is necessary for any PAPR reduction scheme to reduce PAPR without increasing power requirement.
(g) No spectral spillage: The PAPR reduction techniques should not destroy the inherit feature (orthogonality) of OFDM signal.

2.3.1.1 Signal distortion

These methods reduce the PAPR by distorting the OFDM signal non-linearly. The methods like clipping and filtering, peak windowing, and non-linear companding are the example of these techniques. These techniques are applied after the generation of OFDM signal (after the IFFT).

(A) *Clipping and Filtering*

The clipping is the simplest method of PAPR reduction. Clipping limits the maximum amplitude of OFDM signal to a pre-specified level. The implementation of clipping is relatively easy but it has following drawbacks [**135**]:

(a) It causes in-band signal distortion, resulting in BER performance degradation.
(b) It also causes out-of-band radiation, which imposes out-of-band interference signals to adjacent channels. The out-of-band radiation can be reduced by filtering, but the filtering may affect high-frequency components of in-band signal (aliasing) when the clipping is performed with the Nyquist sampling rate.
(c) Filtering after clipping can reduce out-of-band radiation at the cost of peak re-growth. The signal after filtering operation may exceed the clipping level specified for the clipping operation.

To reduce overall peak re-growth, a repeated clipping and filtering can be used to obtain a desirable PAPR at the cost of increase computational complexity [**135**]. Some more techniques have been proposed to cancel out the harmful effects of the amplitude clipping like iteratively clipping and peak windowing. The performance analysis of clipping and filtering process has been given by Ochiai *et. al* in detail [**43**]. The signal to distortion noise ratio (SDR) and channel capacity for clipped OFDM signals has been derived in **[43]**.

(B) *Peak Windowing Method*

It is an improved clipping method. The basic aim of peak windowing is to reduce the out-of-band radiation by using narrow band windows such as Gaussian window to attenuate peak signals. As a matter of fact, any window which is narrow in time domain and having good spectral properties can be used [**102**]. In 2008, an advance peak windowing method has been given by S. Cha *et.al* [**108**] which

overcomes the drawback of normal peak windowing method. It effectively suppresses the peak signals to the desired threshold level in case when the successive peaks occur within a half of the window length.

(C) *Non-Linear Companding*

Non-linear companding is an especial clipping technique which offers good PAPR reduction with better BER performance, low implementation complexity, and no bandwidth expansion. The difference between clipping and companding is that the clipping process deliberately clips the large amplitude signals; therefore the signal cannot be recovered exactly. On the other hand, the companding transform compand the original signals using strict monotone increasing function; therefore the companded signals can be recovered correctly through the corresponding inversion of companding transform at the receiver. Clipping does not affect small amplitude signal, whereas companding enlarge the small signals while compressing the large amplitude signals. A lot of companding techniques are available in the literature. The basic concept of most of the companding techniques is to transform the Rayleigh distributed OFDM signal into a uniformly distributed signal.

The first nonlinear companding transform (NCT) for PAPR reduction was given by Wang *et.al* in 1999 [**134**]. It was based on the speech processing algorithm μ-law and it has shown better performance than that of clipping method [**134**]. The μ-law companding transform mainly focuses on enlarging small amplitude signals while keeping peak signals unchanged, and thus it increase the average power of the transmitted signals and possibly results in exceeding the saturation region of HPA to make the system performance worse. In order to overcome the problem of μ-law companding (increasing average power) and to have efficient PAPR reduction, some more non-linear transform have been suggested in the literature [**13, 56, 123, and 136**].

2.3.1.2 Coding methods

The coding methods employed some error correcting codes for the PAPR reduction. These methods applied before the generation of OFDM signal (before IFFT). When N signals are added with the same phase, they produce a peak power, which is N times the average power. The basic idea of all coding schemes for the reduction of PAPR is to reduce the occurrence probability of the same phase of N signals. The coding method selects such code words that minimize or reduce the PAPR. It causes no distortion and creates no out-of-band radiation, but it suffers from bandwidth efficiency as the code rate

is reduced. It also suffers from complexity to find the best codes and to store large lookup tables for encoding and decoding, especially for a large number of subcarriers.

The first method of PAPR reduction based on coding scheme was given in 1994 by Jones *et.al* [**3**]. This method uses simple block coding scheme. Its basic idea is to map 3 bits data into 4 bits codeword by adding a Simple Odd Parity Code (SOBC) at the last bit across the channels. The main disadvantage of SOBC method is that it can reduce PAPR only for a 4-bit codeword. In 1996, Wulich applied the Cyclic Coding (CC) method to reduce the PAPR [**27**]. In recent years, some more methods have been proposed which uses Golay complementary sequence, Reed Muller code, LDPC codes [**88**] for PAPR reduction. The major drawbacks of all these method are that they significantly reduce the transmission rate.

2.3.1.3 Probabilistic (Scrambling) techniques

The probabilistic methods are based on scrambling of each OFDM symbol with different scrambling sequences and selecting that sequence which gives smallest PAPR. While it does not suffer from the out-of-band power, the spectral efficiency decreases and the complexity increase as the number of subcarriers increases. Also it increases the overhead as side information is required at the receiver. Furthermore, it cannot guarantee the PAPR below a specified level. The methods like Selective Mapping (SLM) and Partial Transmit Sequence (PTS) are the example of probabilistic techniques.

(A) *Selective Mapping (SLM)*

In SLM, the basic idea is to generate a set of OFDM signals, all of them representing the same data block, and then transmitting the one with the lowest PAPR [**95**]. The major drawback of SLM method is that it is more computationally complex because more than one IFFT blocks are used. It also decreases the data rate because the selected signal index, called *side information*, must also be transmitted to allow for the recovery of the original data block at the receiver side. The eventual loss of the side information during transmission significantly degrades the error performance of the system since the whole data block is lost in this case. Therefore, a lot of work has been suggested as a modified SLM to reduce the computational complexity [**24**] and to reduce or to remove the side information transmitted [**118**].

(B) *Partial Transmit Sequence (PTS)*

In PTS, the original data block is divided into multiple non-overlapping sub-blocks. Then these sub-blocks are rotated with rotation factors which are statistically independent. After that, the signal with the lowest PAPR is chosen for transmission. There are several ways for the partition of the data sequence into multiple sub-blocks, including adjacent partition, interleaved partition and pseudorandom partition [**116**]. Among them, pseudo-random partitioning has been found to be the best choice.

Similar to SLM, the major drawback of PTS is also the computational complexity (search complexity for optimal phase factor, and more than one IFFT blocks) and low data rate (required side information). Several techniques have been proposed in the literature to reduce the search complexity and overhead (by reducing/avoiding the usage of side information) **[4].** The complexity of PTS is less than SLM **[96]**.

2.3.1.4 Pre-distortion methods

The pre-distortion methods are based on the re-orientation or spreading the energy of data symbol before taking IFFT. The pre-distortion schemes include DFT spreading, pulse shaping or pre-coding and constellation shaping. The methods like Tone Reservation (TR) and Tone Injection (TI) are the example of constellation shaping schemes.

(A) *Tone Injection (TI) and Tone Reservation (TR)*

The TR and TI are two efficient techniques of PAPR reduction which are based on the reorientation (shaping) of constellation before the OFDM modulation. The key idea is that both transmitter and receiver reserve a subset of tones for generating PAPR reduction signals. These tones will not be used for data transmission. In TR, the objective is to find the time domain signal $c(i,n)$ to be added to the original OFDM signal $x(i,n)$ to reduce the PAPR [**122, 139**]. The resultant OFDM signal can be written as-

$$\tilde{x}(i,n) = IFFT\ (\ X(i,k) + C\ (i,k)\ ) = x(i,\ n) + c(i,\ n)\ , \qquad \textbf{(2.3.1.1)}$$

where, $c(i,n) = IFFT(C(i,k))$ and $X(i,k)$ is the complex data symbol.

Therefore, the main task of any TR scheme is to find out the proper $C(i,k)$ to make the output $\tilde{x}(i,n)$ with low PAPR. The value of $C(i,k)$ can be determined with the help of any convex optimization algorithm or with the help of linear programming methods.

The basic idea of TI is to extend the constellation size so that each of the points in the original constellation can be mapped into several equivalent points in the expanded constellation. Since each symbol in a data block can be mapped into one of several equivalent constellation points, these extra degrees of freedom can be exploited for PAPR reduction. This method is called tone injection because substituting a point in the basic constellation for a new point in the larger constellation is equivalent to injecting a tone of the appropriate frequency and phase in the multicarrier signal. The main advantage of TI is that it does not require the extra side information and the receiver only needs to know how to map the redundant constellations on the original one.

Some modifications of TI have been proposed to obtain good performance including PAPR reduction and low complexity [**74, 110, and 128**]. This technique is called active constellation extension (ACE). In this technique, some of the outer signal constellation points in the data block are dynamically extended toward the outside of the original constellation such that the PAPR of the data block is reduced. The constellation points are extended such that the PAPR is minimized but the minimum distance of the constellation points does not decrease. The TI technique is more problematic than the TR technique since the injected signal occupies the frequency band as the information bearing signals. Moreover, the alternative constellation points in TI technique have an increased energy and the implementation complexity increases for the computation the optimal translation vector.

(B) *Pulse Shaping or Pre-coding*

The pulse shaping or pre-coding technique is an efficient and flexible way for reducing the PAPR of OFDM signals. In this method, each data block is multiplied by a pre-coding matrix prior to OFDM modulation and transmission. This method is data-independent and, thus, avoids block based optimization. It also works with an arbitrary number of subcarriers and any type of baseband modulation used. In terms of BER performance, it takes advantage of the frequency variation of the fading-multipath channel and improves the BER of OFDM signals in comparison to conventional OFDM (no pre-coding). The implementation complexity of the proposed technique is acceptable, since a predefined pre-coding matrix is used and thus, no handshake is needed between transmitter and receiver. Having the same pre-coding matrix for all OFDM blocks avoids all the processing needed in block-based optimization methods. In 1998, S.B. Slimane proposed a pulse shaping method for PAPR reduction and

later in 2007; he again proposed pulse shaping as a pre-coding technique for PAPR reduction [**105**]. In this paper, he proposed an efficient design procedure for generating pre-coding matrix. Subsequently, Hao *et.al* in 2010 [**75**], derived a necessary condition and proposed a systematic procedure to generate an optimal pre-coding matrix which will give minimum bit error rate. In the pre-coding scheme, the design of pre-coding matrix plays an important role.

2.3.1.5 Hybrid techniques

Besides these different PAPR reduction techniques, some hybrid methods are also available in the literature [**5, 15, and 114**]. These methods combine two or more than two techniques for PAPR reduction like clipping with coding, SLM with coding, pre-coding with clipping etc. The hybrid methods are considered as better choice for PAPR reduction because it posses the advantages of both techniques used in hybridization with slight increases in complexity.

2.3.2 Performance Comparison of Different PAPR Reduction Techniques

A number of techniques which were developed in last two decades to combat the PAPR problem in OFDM systems have been discussed. It is clearly understood from above discussion, that although the target is same but a lot of diverse approaches have been applied. Each and every scheme reduces the PAPR but also exhibits some drawbacks (in terms of complexity, bandwidth increases etc.). Hence there is no consensus over the best solution for the problem at hand.

An OFDM system with 256 subcarriers and 16-QAM constellation with the oversampling rate of 4 are used for the performance comparison of different PAPR reduction techniques **[122]**. The preset clipping level A has been selected to 80% of the maximum of the original OFDM symbols in the clipping scheme and the number of the reserved tone is 20 in TR scheme. For PTS scheme, the rotation vectors belong to the set {+1,-1} and the number of the sub-blocks is 16. Therefore, the 215 searches are for each optimal PTS. For nonlinear companding transform, the exponential companding is used.

Figure-2.3.2.1 shows the complementary cumulative distributive function (CCDF) plot of different PAPR reduction techniques. All methods have great ability of PAPR reduction, but their performance is different as clearly visible form CCDF plots. As visible from plots that the signals companded by the exponential companding transform function can reduce the PAPR largest and the PAPR reduction of the clipping scheme is the smallest among these typical methods. Although clipping

scheme can improve its performance of the PAPR reduction through reducing its preset clipping level ('A'). However, the performance of the BER will be degraded largely when its preset clipping level is reduced **[43]**.

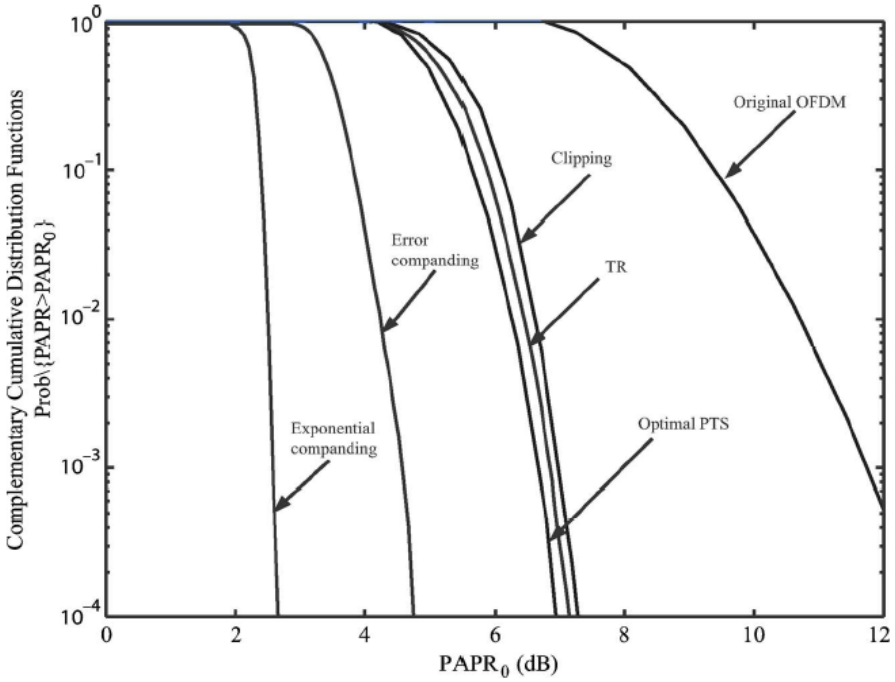

Figure-2.3.2.1: CCDF comparisons of different PAPR reduction methods [122]

At the end, the comparison between different PAPR reduction techniques is given in the Table- 2.1. Similar comparison is given in [**122**], but this comparison also includes the pre-coding technique. The comparison is made on the basis of five factors like average power, computational complexity, bandwidth expansion, BER performance, and Side information required.

Table-2.1: Comparison between different PAPR reduction techniques.

Methods	Average Power	Computational Complexity	Bandwidth Expansion	BER Degradation	Side Information
Clipping	No	Low	No	Yes	No
NCT	No	Low	No	Yes	No
Coding	No	Low	Yes	No	No
PTS/SLM	No	High	Yes	No	Yes
TR/TI	Yes	High	Yes	No	No
Pre-coding	No	Low	Yes	No	No

2.4 SYNCHRONIZATION

One of the major disadvantages of OFDM system is its sensitivity to synchronization errors (time and frequency) at the receiver. At the receiver, there exist carrier-frequency offset (CFO), sampling clock errors, and symbol-timing offset (STO). Inaccurate estimation of timing and carrier frequency offset destroys the orthogonality among sub-carriers and generates ICI and inter-symbol interference (ISI) [**78, 83, and 126**]. All these offsets must have to be estimated and compensated before taking the FFT of received signal. Usually the frequency offset and timing errors are more dominant than the sampling clock inaccuracy. The effect of STO and CFO are discussed in following sections.

2.4.1 Effect of Symbol Timing Offset

The timing synchronization in multi-carrier (i.e., OFDM) system is significantly different than for a single carrier system. In multi-carrier system there is not an "eye opening" where a best starting time sample can be found. Rather there are hundreds or thousands of samples per OFDM symbol since the number of samples necessary is proportional to the number of subcarriers. The main aim of symbol timing estimator in an OFDM system is to find the start of OFDM symbol or in other words to find the starting point of FFT window.

Considering the sample indices of a perfectly synchronized OFDM symbol are $\{-G, -G+1, \ldots, -1, 0, 1, \ldots, N-1\}$ and the maximum channel delay spread is $\tau_{\max}$. Let the starting point of FFT window decided by the timing estimation method is at the sample $\mathrm{r}(\delta)$, where $'\delta'$ is an integer-valued STO. Then, if timing offset $'\delta'$ lies in the region $\{-G+\tau_{max}, -G+\tau_{max}+1, \ldots, 0\}$, the orthogonality among the sub-carriers will not be destroyed and the timing offset will only introduced a phase rotation. The output of FFT in this case can be written as-

$$Y(i,p) = \exp\left(\frac{j\,2\,\pi\,p\,\delta}{N}\right)\; X(i,p)\; H(p) + W(i,p), \quad for \;\; -G+\tau_{max} \leq \delta < 0 \qquad \textbf{(2.4.1.1)}$$

where, $H(p)$ is the channel frequency response for the p^{th} sub-carrier. This phase rotation can be compensated by a one tap perfect channel equalizer.

If the timing offset $'\delta'$ lies outside the above range then it generates ISI and ICI at the output of FFT. The output of FFT in this case can be written as [**83**] –

$$Y(i,p) = \frac{N-\delta}{N} X(i,p) \; H(i,p) \; e^{j\,2\pi\,p\,\delta\,/\,N} + \underbrace{\frac{1}{N}\sum_{k=0,k\neq p}^{N-1} X(i,k) \; H(i,k)\, e^{j\,2\pi\,k\,\delta\,/\,N} \left\{\sum_{n=0}^{N-1-\delta} 1 \times e^{\frac{j\,2\pi\;n\,(k-p)}{N}}\right\}}_{ICI} + \underbrace{\frac{1}{N}\sum_{k=0}^{N-1} X(i+1,k) \; H(i+1,k) \; e^{j\,2\pi\,k\,(n+\delta-G-N)\,/\,N} \left\{\sum_{n=N-\delta}^{N-1} 1 \times e^{\frac{-j\,2\pi\;p\,n}{N}}\right\}}_{ISI} + W'(i,p),$$

$$for \quad p = 0, 1, \ldots, N-1 \qquad \textbf{(2.4.1.2)}$$

The first term in (2.4.1.2) indicates that timing offset results in phase offset and attenuation of k^{th} sub-carrier output of i^{th} OFDM symbol. The second additive term represents ICI while the third term stands for ISI. The last term represents the AWGN.

2.4.2 Effect of Carrier Frequency Offset

The CFO is caused by the misalignment in carrier frequencies or due to Doppler shift arises by channel [**83, 119**]. The received signal given in (2.2.4.1) has considered only the effect of multipath fading channel. Therefore, including the effect of CFO along with effects of multipath fading channel and after CP removal, the samples of i^{th} received signal analogous to (2.2.4.1) can be expressed as –

$$r(i,n) = \exp\left(\frac{j\,2\pi\,n\,\epsilon}{N}\right) \sum_{l=0}^{L-1} h_l(n)\, \tilde{x}(i, n-\tau_l) + w(i,n),$$

$$for \quad n = 0, 1, \ldots, N-1 \qquad \textbf{(2.4.2.1)}$$

where, $'\varepsilon'$ is the carrier-frequency offset normalized by the sub-carrier spacing $(1/T_u = 1/NT_s)$, $h_l(n)$ is the impulse response of frequency selective multipath fading channel with path gains $\{h_l(n):$

$l = 0,1,\dots,L-1\}$, τ_l is the path delay of l^{th} path, and $w(i,n)$ is a zero-mean, complex value Gaussian noise process with variance σ_w^2. Let consider a perfect timing synchronization (i.e. timing offset δ = 0). The output of FFT in this case is given as –

$$Y(i,p) = \frac{1}{N}\sum_{k=0}^{N-1} X(i,k)\,H(k)\,S(k-p+\varepsilon) + W(i,p),$$

$$for\ p = 0,1,\dots,N-1 \qquad \textbf{(2.4.2.2)}$$

After breaking the summation in two terms –

$$Y(i,p) = \frac{1}{N}X(i,p)\,H(p)S(\varepsilon) + \underbrace{\frac{1}{N}\sum_{\substack{k=0,\\ k\neq p}}^{N-1} X(i,k)\,H(k)\,S(k-p+\varepsilon)}_{ICI} + W(i,p),$$

$$for\ p = 0,1,\dots,N-1 \qquad \textbf{(2.4.2.3)}$$

where, $H(k)$ is frequency response of channel to the k^{th} subcarrier and $S(k-p+\varepsilon)$ is an ICI coefficient, which is defined as –

$$S(k-p+\varepsilon) = \sum_{n=0}^{N-1} 1 \times e^{\frac{j\,2\,\pi\ n\,(k-p+\varepsilon)}{N}},$$

$$= e^{j\,\pi\,(k-p+\varepsilon)\frac{N-1}{N}}\ \frac{Sin(\,\pi\,(k-p+\varepsilon))}{Sin(\,\pi\,(k-p+\varepsilon)/\,N)},$$

(2.4.2.4)

$$S(\varepsilon) = \sum_{n=0}^{N-1} 1 \times e^{\frac{j\,2\,\pi\ n\,\varepsilon}{N}},$$

$$= e^{j\,\pi\,\varepsilon\frac{N-1}{N}}\ \frac{Sin(\,\pi\,\varepsilon)}{Sin(\,\pi\,\varepsilon/\,N)} = \begin{cases} N, & for\ \varepsilon = 0 \\ Non\ Zero, & for\ \varepsilon \neq 0 \end{cases}$$

(2.4.2.5)

The first term in the above equation represents the desired symbol with amplitude distortion due to frequency offset. The second term represents the ICI from other subcarriers into p^{th} subcarrier frequency component, which implies that the orthogonality among subcarrier frequency components is not maintained any longer due to the frequency offset. The last term is AWGN.

The main task of synchronization is to estimate and compensate the timing offset ($'\delta'$) and the frequency offset ($'\varepsilon'$). The estimation is achieved in two steps through the use of training symbol, which will usually be placed at the start of the frame. First, the timing estimation is performed based on the timing metric. This timing estimation gives the start position of training symbol. Then, this estimated training symbol is used for frequency offset estimation.

2.4.3 Timing and Frequency Offset Estimation Methods

Several methods are available in the literature for estimating the time and frequency offset. These methods are broadly classified as (a) Data Aided (DA), (b) Non Data Aided (NDA). The DA method uses training symbols whereas NDA method uses either cyclic prefix or blind techniques for synchronization.

The DA methods [**1, 2, 6, 17, 19, 20, 35, 36, 41, 42, 66, 71, 79, 81, 92, 107, 125 and 142]**, have high accuracy and low implementation complexity therefore these methods are more suitable for packet oriented applications which requires fast and reliable synchronization such as IEEE 802.11(a) and HIPERLAN/2. However, their bandwidth efficiency is reduced due to large overhead. On the other hand NDA methods [**57, 97, and 115**] have high implementation complexity and less overhead therefore the NDA methods are more suitable for continuous transmission like DVB-T [**102, 113, and 78**]. The estimation range of non-data aided methods is too small therefore not suitable for acquisition.

2.4.3.1 Timing offset estimation methods

In DA methods, for timing synchronization [**1, 6, 17, 41, 42, 66, and 125**], a preamble is transmitted which consists of some repetitive blocks and then applying a sliding window correlator or matched filter at the receiver to detect the maximum of timing metric. The output of the correlator or matched filter is expected to exhibit a peak when the sliding window is perfectly aligned with the received training symbol block. The timing metric with sharp peak is preferred for the better timing estimation.

The most popular DA method for timing synchronization was given by T. M. Schmidl and D .C. Cox [**125**]. The training symbol of Schmidl & Cox has two identical halves to estimate the symbol timing offset. However, its timing metric exhibits a large plateau which causes a large variance in timing

estimation. In order to reduce the variance, lot of methods has been suggested in the literature with sharper timing metric and less variance.

Similar to structure given by Schmidl & Cox, Coulson's algorithm uses two repeated m-sequences as a training symbol for timing synchronization **[6]**. However, the Coulson's synchronization scheme fails in the presence of large frequency offset and is highly computationally complex due to the matched filtering. Minn *et.al* [**41**] had proposed a training symbol with more than two identical segments along with flipping the signs of last two segments to obtain a steeper roll-off trajectory at the correct timing position in the timing metric. Minn's algorithm uses autocorrelation on both halves and sums the results, which gives a sharper peak.

Subsequently, Park *et.al* [**17**] proposed a different timing synchronization scheme based on reverse auto-correlation method and achieved a sharper timing metric than Schmidl & Cox and Minn's method. It performs better than Schmidl & Cox and Minn *et.al* in slow fading channel but its performance degraded in strong fading channel. In the same year, Minn *et.al* [**42**] had been extended their previous work [**41**] by introducing more symbol pattern for timing synchronization. Later on, K. Shi and E. Serpedin [**66**] modified the Minn's scheme with outcome of a more advanced timing metric based on the maximum likelihood criterion.

In order to further reduce the uncertainty in the timing offset estimation, Awoseyila *et.al* [**1, 2**] had introduced an improved timing estimation scheme based on the combination of auto-correlation and cross-correlation methods. The variance of timing offset with Awoseyila *et.al* method is less than all other methods discussed above in strong fading channel.

2.4.3.2 Frequency offset estimation methods

In DA methods, for frequency offset estimation [**2, 35, 36, 71, 79, 107, 125, and 142**], the CFO is usually divided in two parts (a) the fractional frequency offset (FFO); (b) the integer frequency offset (IFO). In the year 1994, P. H. Moose gave first preamble based CFO estimation algorithm **[92]**. Moose's algorithm was based on maximum likelihood (ML) estimation in frequency domain using two identical training symbols. The acquisition range of Moose's method was ± 1/2 times the sub-carrier spacing. This range can be extended by using shorter symbol with more than two identical parts but at the price of reduced estimation accuracy.

Later, in the year 1997, Schmidl & Cox [**125**] suggested a modified CFO estimation method using two training symbols with differential encoding at identical subcarrier positions. The performance of Schmidl & Cox method was better than Moose estimator both in terms of accuracy and acquisition range. The first symbol which consists of two identical halves was used for FFO estimation whereas IFO was estimated in frequency domain by using second symbol. The estimation range of Schmidl & Cox was ± N/2 times the subcarrier spacing, for FFT size of N.

To reduce the overhead due to second symbol in Schmidl & Cox method, Morelli *et.al* [**79**] introduced the best linear unbiased estimator (BLUE) as an extension of Schmidl & Cox method. Morelli's method consists of one training symbol with $'\mathcal{M}'$ identical parts to achieve improved frequency accuracy in the time domain; however, its estimation range is only $\pm\mathcal{M}/2$ times the subcarrier spacing which is less than Schmidl & Cox. Furthermore, the Morelli's algorithm can estimate integral and fractional part of frequency offset simultaneously and is reported to have a lower frequency offset estimation variance than Schmidl & Cox at the cost of computational complexity.

Similar to Schmidl & Cox method, Zhang *et.al* [**142**] has also used two symbols for frequency offset estimation employing ML estimator. Zhang has reported low estimation variance than Schmidl & Cox method **[125]** at the cost of high complexity, whereas its acquisition range is ± N/4 times the sub-carrier spacing which is less than [**125**]. In the same year, Shi and Serpedin [**66**] had also presented a coarse CFO estimator using only one symbol consists of four identical parts with the pattern of sign change similar to Minn *et.al* method [**41**]. The acquisition range of Shi and Serpedin method is only ± 2 whereas the mean square error (MSE) performance is comparable to Schmidl & Cox method.

Motivated by the usefulness of constant envelope preamble in synchronization, Ren *et.al* [**35**] had introduced a new synchronization method based on constant amplitude zero auto-correlation (CAZAC) training symbols with two identical parts, weighted by a binary pseudo-random noise (PN) sequence. Ren's timing algorithm was based on differential cross-correlation of a randomized sequence, using a differential lag of N/2. The performance of Ren's method in timing synchronization is better than Park *et.al* method [**17**] at lower SNR whereas comparable at higher SNR. For frequency synchronization, its performance is better than Morelli *et.al* method [**79**] at lower SNR whereas comparable at higher SNR. The frequency offset acquisition range in Ren's method was reported as ± N/2 the sub-carrier spacing, better than Morelli *et.al* method. Subsequently, in the year 2007, Wei *et.al* [**71**] had suggested an improved synchronization method based on CAZAC sequences for integer frequency offset. The performance of this method was reported better than Schmidl & Cox method in terms of probability of failure.

2.4.4 Performance Comparison of Different Estimation Methods

In this section, the performance of different timing and frequency offset estimator is compared using simulation method. For timing offset estimation, the performance of Schmidl & Cox **[125]**, Minn *et.al* **[41]**, Park *et.al* **[17]**, Shi & Serpedin **[66]**, and Awoseyila *et.al* **[1]** has been considered. Similarly for frequency estimator, the method given by Schmidl & Cox **[125]**, Morelli *et.al* **[79]**, and Wei *et.al* **[71]** has been considered. For this comparison, an OFDM system with 256 sub-carriers and 16 cyclic prefix with QPSK modulation is simulated. An ISI channel model **[55, 127]**, consisting of $L = 8$ paths with path delays of $m_i = 0, 1, \ldots, L-1$ samples and an exponential power delay profile having average power of $e^{-m_i/L}$ is used, wherein each path undergoes independent Rayleigh fading. The MSE has been taken as performance evaluation parameter.

The comparison of MSE of timing offset with all estimators considered above in the multipath fading channel described above is shown in Figures-2.4.4.1. It is clearly visible from Figure-2.4.4.1 that the values of MSE of timing offset with Awoseyila *et.al* method are much better as compared to other estimators.

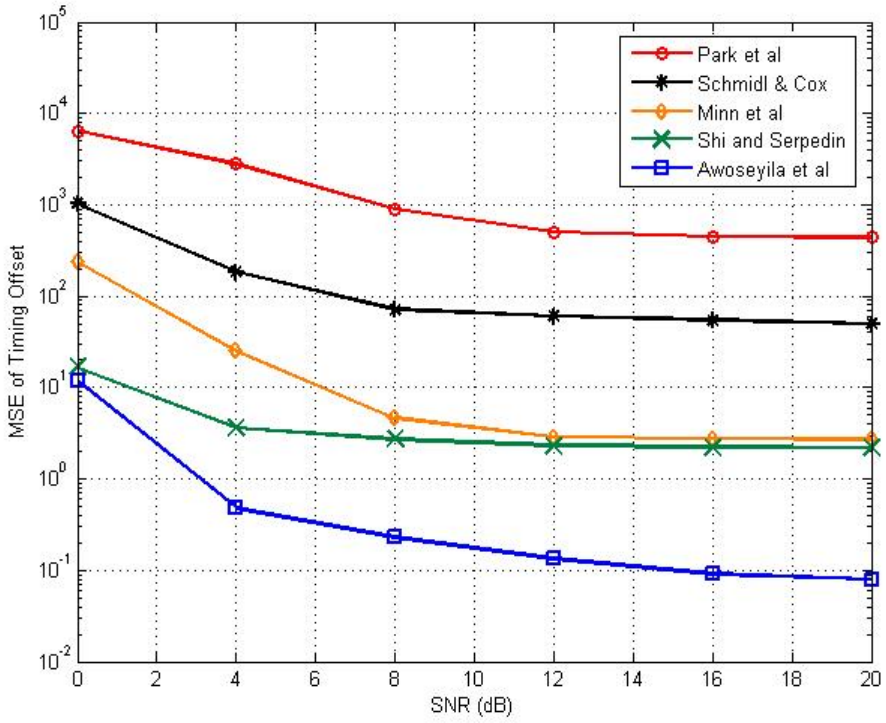

Figure-2.4.4.1: Comparison of different timing offset estimator in fading channel

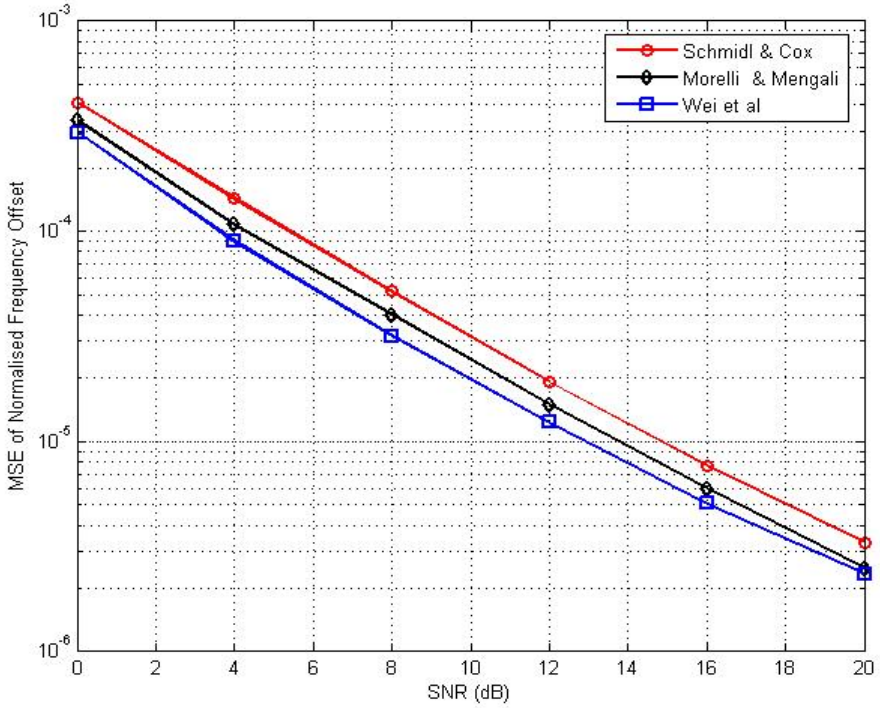

Figure-2.4.4.2: Comparison of different frequency offset estimator in fading channel

Similarly, the comparison of MSE of frequency offset with all estimators considered above in the multipath fading channel is shown in Figure-2.4.4.2. In the case of frequency offset estimation, the method given by Wei *et.al* outperforms all other method, as visible in Figure-2.4.4.2.

2.5 ICI REDUCTION TECHNIQUES

The effect of CFO in the OFDM system has been discussed in section-2.4.2 and it has been found that due to CFO, the ICI is generated at the output of FFT block which degrades the performance of OFDM system [**83**] and [**22, 54, 64**]. CFO can be compensated by frequency offset estimation techniques discussed above in section-2.4.3.2. However, estimation error is inevitable, and the residue frequency offset usually exists in OFDM systems. Therefore, it is of interest to investigate schemes that are robust to frequency offset. Several techniques have been introduced in the past to reduce ICI. These include frequency domain equalization [**53, 85**], self cancellation scheme [**84, 140**], and windowing technique (pulse shaping at the transmitter and receiver windowing) [**25, 26, 65, 86, 87, 94, 99, 111, and 129**].

2.5.1 Windowing Method for ICI Reduction

A lot of work has been published in literature which described the use of windowing in OFDM system for ICI reduction. These works can be classified in two groups. One groups used windowing or pulse shaping at the transmitter side and another groups suggested the use of windowing at the receiver side.

At transmitter side, the OFDM signal after IFFT is cyclically extended and then the windowing is applied in such a way so that it affects only CP part of the signal, and original part remains unchanged. The basic aim of windowing at the transmitter is to make the spectrum go down rapidly. Windowing an OFDM symbol makes the amplitude go smoothly to zero at the symbol boundaries. On the other hand if windowing is not used than the out-of-band spectrum decreases rather slowly because of sharp phase transition at symbol boundaries. The IEEE 802.11 standards have given the use of raised-cosine (RC) window at transmitter side. Several other pulse shapes are also available in the literature [**86, 87, 94, 99, and 129**].

On the other hand, the receiver windowing is used to reduce the sensitivity to frequency errors. The concept of receiver windowing for ICI reduction has been described in [**25, 86 and 111**]. In receiver windowing, the received signal is multiplied by the time domain window and then the FFT of that multiplied signal has been taken. It has been shown in [86], that the use of a proper Nyquist window will reduce the ICI drastically. Several Nyquist pulse shapes are available in the literature like RC, "better than" raised-cosine (BTRC), Frank's window (FRANK), Second Order Continuous Window (SOCW), double jump window, Sinc Power Pulse (SP), Improved Sinc Power Pulse (ISP) and Phase Modified Sinc Pulse (PMSP). The expression of ICI power and Signal to Interference Ratio (SIR) for q^{th} sub-carrier, when using windowing method (either as transmitter side or at receiver side) is given as **[94]**-

$$\sigma_{ICI_q}^2 = \sum_{r=0, r \neq q}^{N-1} |P(r-q+\varepsilon)|^2 \qquad \textbf{(2.5.1)}$$

$$SIR_q = \sigma_s^2 \,/\, \sigma_{ICI_q}^2 = |P(\varepsilon)|^2 \Big/ \sum_{k=0,\ k\neq 0}^{N-1} |P(k-q+\varepsilon)|^2 \qquad \textbf{(2.5.2)}$$

where, $P(f)$ is the Fourier transform of pulse shape $p(t)$ and σ_s^2 is power of desired signal.

It is clear from (2.5.1), that the average ICI power for the q^{th} symbol depends on the number of subcarriers and on the spectral magnitudes of the pulse-shaping function at the frequencies $(r - q + \varepsilon), r \neq q, r = 0,1,2, \ldots N - 1$. For the window function which follows Nyquist criteria have nulls at the frequency points $(r - q)/N$, and hence no ICI occurs, when $\Delta f = 0$.

2.5.1.1 Different window functions

Several window functions or pulse shaping function have been proposed in the literature for ICI reduction. One important condition required for any pulse shaping function is that the Fourier transform of the pulse $p(t)$ should have spectral nulls at the frequencies $\pm 1/T$, $\pm 2/T$, ... to ensure sub-carrier orthogonality. The pulse shapes which full-fill this requirement is called Nyquist pulse shape. From the studies, it is found that the pulse shapes like RC, BTRC, SOCW, and FRANK have been used in receiver windowing and other pulse shapes like SP, ISP, and PMSP have been used at transmitter side only.

From the literature survey, it has been found that no closed-form expressions in time domain are available for the pulse shapes like SP, ISP and PMSP. However, these pulse shapes can be evaluated in time domain through a numerically using IFFT. On the other hand, the expression of RC, BTRC, SOCW, and FRANK are available both in time domain and in frequency domain. The expression of different pulse shapes in time and frequency domain is given below:

(A) *Rectangular Window (RT)*

$$p_{rt}(t) = \begin{cases} \frac{1}{T}, & -\frac{T}{2} \leq |t| \leq \frac{T}{2} \\ 0, & otherwise \end{cases} \quad \textbf{(2.5.3)}$$

$$P_{rt}(f) = Sinc(fT) \quad \textbf{(2.5.4)}$$

(B) *Raised-Cosine (RC)*

$$p_{rc}(t) = \begin{cases} \frac{1}{T}, & 0 \le |t| \le \frac{T(1-\alpha)}{2} \\ \frac{1}{2T}\left\{1 + Cos\left[\frac{\pi}{\alpha T}\left(|t| - \frac{T(1-\alpha)}{2}\right)\right]\right\}, & \frac{T(1-\alpha)}{2} \le |t| \le \frac{T(1+\alpha)}{2} \\ 0, & otherwise \end{cases}, \quad \textbf{(2.5.5)}$$

$$P_{rc}(f) = Sinc(fT)\ \frac{Cos\,(\pi\ \alpha\ f\ T)}{1 - (2\ \alpha\ f\ T)^2} \quad \textbf{(2.5.6)}$$

(C) *Better Than Raised Cosine (BTRC)*

$$p_{btrc}(t) = \begin{cases} \frac{1}{T}, & 0 \le |t| \le \frac{T(1-\alpha)}{2} \\ \frac{1}{T}\ exp\left\{-\frac{2\ log\,2}{\alpha T}\left(|t| - \frac{T(1-\alpha)}{2}\right)\right\}, & \frac{T(1-\alpha)}{2} \le |t| \le \frac{T}{2} \\ \frac{1}{T}\left\{1 - exp\left\{-\frac{2\ log\,2}{\alpha T}\left(\frac{T(1+\alpha)}{2} - |t|\right)\right\}\right\}, & \frac{T}{2} \le |t| \le \frac{T(1+\alpha)}{2} \\ 0, & otherwise \end{cases}, \quad \textbf{(2.5.7)}$$

$$P_{btrc}(f) = Sinc\,(fT)\ \frac{2\,\beta'\,f\,T\,Sin\,(\pi\,\alpha\,f\,T) + 2\,Cos\,(\pi\,\alpha\,f\,T) - 1}{1 - (2\,\beta\,f\,T)^2} \quad \textbf{(2.5.8)}$$

where, $\beta' = \alpha\,\pi\ /\ log_e(2)$

(D) *The Frank Pulse*

$$p_{frank}(t) = \begin{cases} 1, & |t| \le \frac{T(1-\alpha)}{2} \\ 1 - \frac{|t|}{T}, & \frac{T(1-\alpha)}{2} \le |t| \le \frac{T(1+\alpha)}{2} \\ 0, & otherwise \end{cases} \quad \textbf{(2.5.9)}$$

(E) *The Second Order Continuous Window (SOCW)*

$$p_{socw}(t) = \begin{cases} 1, & |t| \le \frac{T(1-\alpha)}{2} \\ 1 - f\left(-\frac{2|t|}{\alpha T} + \frac{1}{\alpha}\right), & \frac{T(1-\alpha)}{2} \le |t| \le \frac{T}{2} \\ f\left(\frac{2|t|}{\alpha T} - \frac{1}{\alpha}\right), & \frac{T}{2} \le |t| \le \frac{T(1+\alpha)}{2} \\ 0, & otherwise \end{cases} \quad \textbf{(2.5.10)}$$

where, $f(t) = 0.5 + a_1 t + a_2 t^2$ *and* $a_2 = -0.5 - a_1$

$$P_{socw}(f) = Sinc(fT)\left[2(1+a_1)\,Sinc(\alpha fT) - (1+2a_1)\,Sinc^2\left(\frac{\alpha fT}{2}\right)\right] \quad \textbf{(2.5.11)}$$

where, α is a roll-off factor which is lies in the range of 0 to 1.

Some pulse shapes are defined only in frequency domain like:

(F) *The Sinc Power Pulse (SP)*

$$P_{SP}(f) = Sinc^{n}(fT) \tag{2.5.12}$$

(G) *The Improved Sinc Power (ISP) Pulse*

$$P_{ISP}(f) = \exp(-a\,(f\,T)^{2})\,Sinc^{n}(fT) \tag{2.5.13}$$

(G) *The Phase Modified Sinc Power Pulse (PMSP)*

$$P_{PMSP}(f) = \exp(-a\,(f\,T)^{2})\,Sinc^{n}\left(\left(f - b\,Sinc(c\,\pi\,f)\right)T\right) \tag{2.5.14}$$

where, $'a'$ is a design parameter to adjust the amplitude , $'n'$ is degree of Sinc function, and parameters $'b'$ and $'c'$ are used to control the phase of the Sinc function. The time domain and frequency domain plots of different window functions which are defined above are shown in Figure-2.5.1 and Figure- 2.5.2 respectively for roll-off factor $\alpha = 1$. The magnitude plots in dB of all pulse shapes are shown in Figure-2.5.3. Similarly, the plots of pulse shapes like *RC, BTRC, SOCW, and FRANK* for roll-off factor $\alpha = 0.5$ are shown in Figure- 2.5.4, Figure- 2.5.5, and Figure- 2.5.6. The pulse shapes like SP, ISP, and PMSP are defined only for roll-off factor $\alpha = 1$, therefore their plots are shown only for $\alpha = 1$.

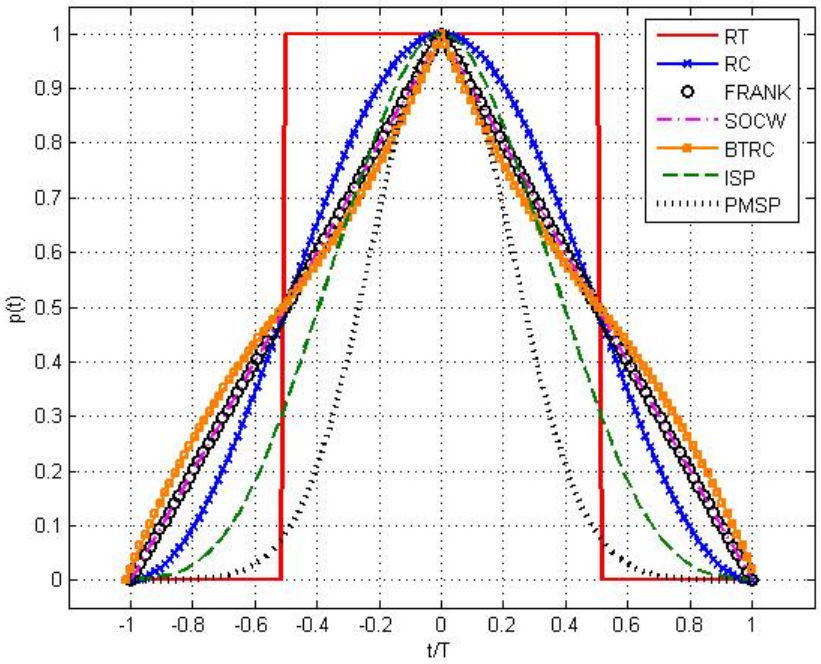

Figure-2.5.1: Time domain plots of different window function at $\alpha = 1$

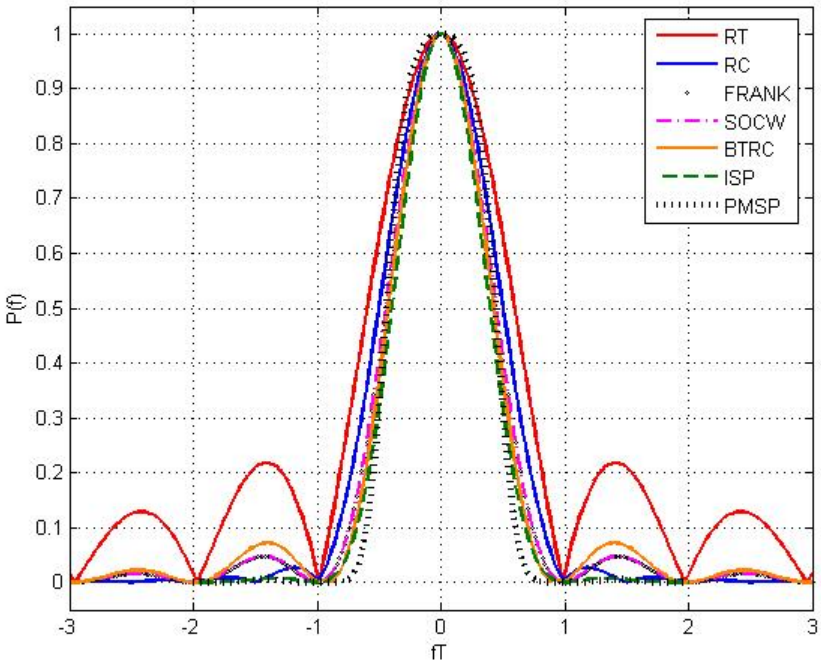

Figure-2.5.2: Frequency domain plots of different window function at $\alpha = 1$

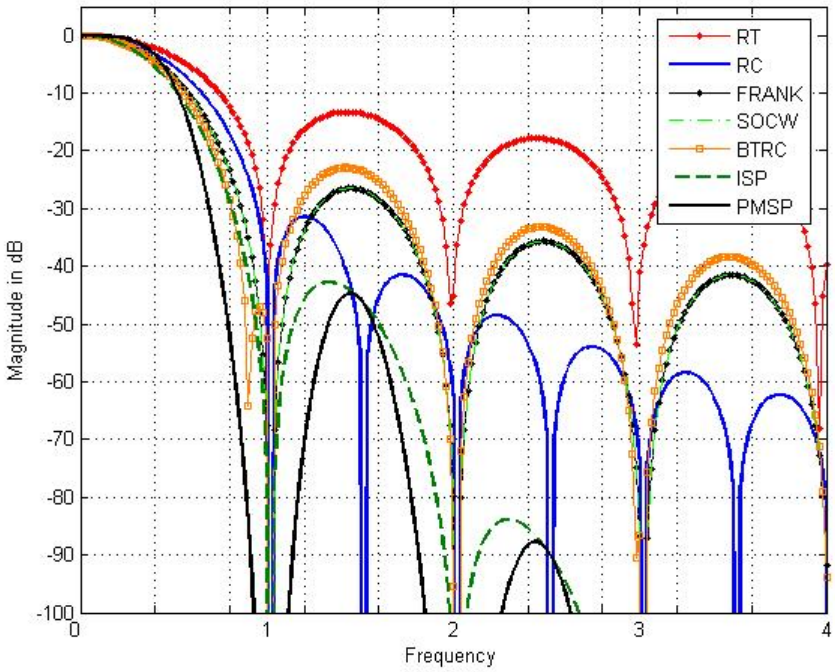

Figure-2.5.3: Magnitude plots in dB of different window function at $\alpha = 1$

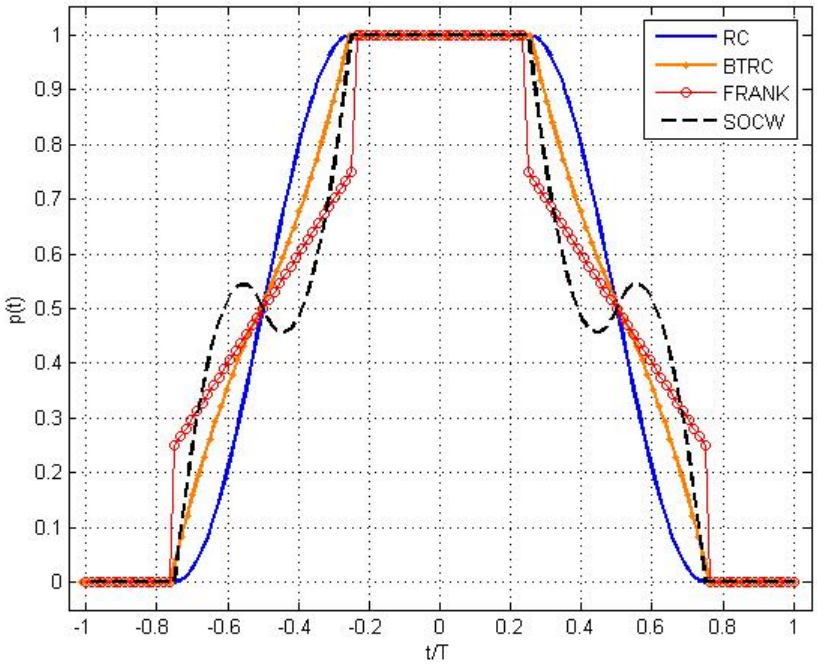

Figure-2.5.4: Time domain plots of different window function at $\alpha = 0.5$

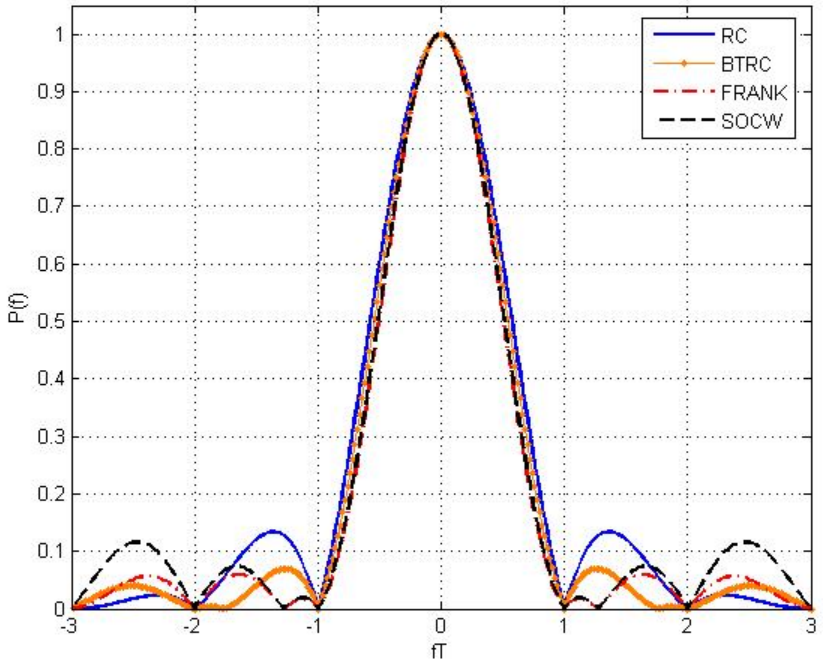

Figure-2.5.5: Frequency domain plots of different window function at $\alpha = 0.5$

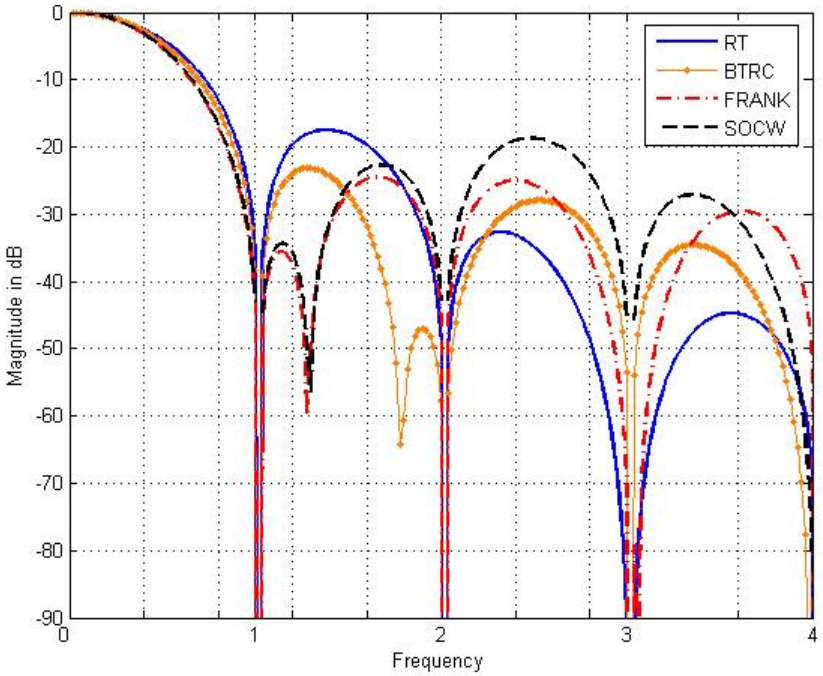

Figure-2.5.6: Magnitude plots in dB of different window function at $\alpha = 0.5$

2.5.1.2 Performance comparison

In this section, the performances of different window functions are compared in terms of ICI power and SIR. Figure- 2.5.7 and Figure- 2.5.8 shows the average ICI power of a 64-subcarrier OFDM system with respect to the normalized frequency offset (ε) for α = 1 and 0.5 respectively. The parameters considered for different window functions are given as-

(a) For SOCW: when $\alpha = 1, a_1 = -0.5$, and when $\alpha = 0.5$, $a_1 = 0.4$

(b) For ISP: $n = 2$, $a = 1$

(c) For PMSP: $n = 2$, $a = 1, b = 0.5$, and $c = 2$

It is clearly visible from **(2.5.1)** that the average ICI power depends on the total number of sub-carriers and on the side lobe level of the window function. Hence, if the spectrum of one pulse-shaping function has smaller side-lobes than another, then it is expected that this pulse shaping function will lead to less ICI. The plots of ICI for different window functions also confirm this analysis.

As visible from Figure-2.5.7, the PMSP pulse shapes outperforms all other window function for α = 1 because its side lobe level is very less in comparison to other pulse shapes as shown in Figure-2.5.2 and Figure- 2.5.3. However, it is defined only for α=1 and hence it cannot be compared with other pulse shapes for $\alpha \neq 1$. Similarly, the ISP is also defined only for $\alpha = 1$. In the case of 'α' other than 1 ($\alpha = 0.5$), the FRANK pulse gives minimum ICI power whereas RC gives the maximum for all value of frequency offset, as visible from Figure 2.5.8. The same analysis can also be done with the help of SIR plots as shown in the Figure 2.5.9 and 2.5.10 for $\alpha = 1$ and $\alpha = 0.5$ respectively.

The side lobe level of any pulse shape is also depends on the roll-off factor 'α', and hence as the 'α' increases from 0 to 1, the side lobe level decreases. This further decreases the ICI power. This phenomenon is visible from Figure- 2.5.7 and Figure- 2.5.8. For example, consider the case of BTRC pulse shapes, at $\alpha = 1$ and $\varepsilon = 0.1$, the ICI power is $-33.45\ dB$ and at $\alpha = 0.5$ and $\varepsilon = 0.1$, the ICI power is $-21.45\ dB$. The ICI power reduces 12 dB as 'α' increases from 0.5 to 1.

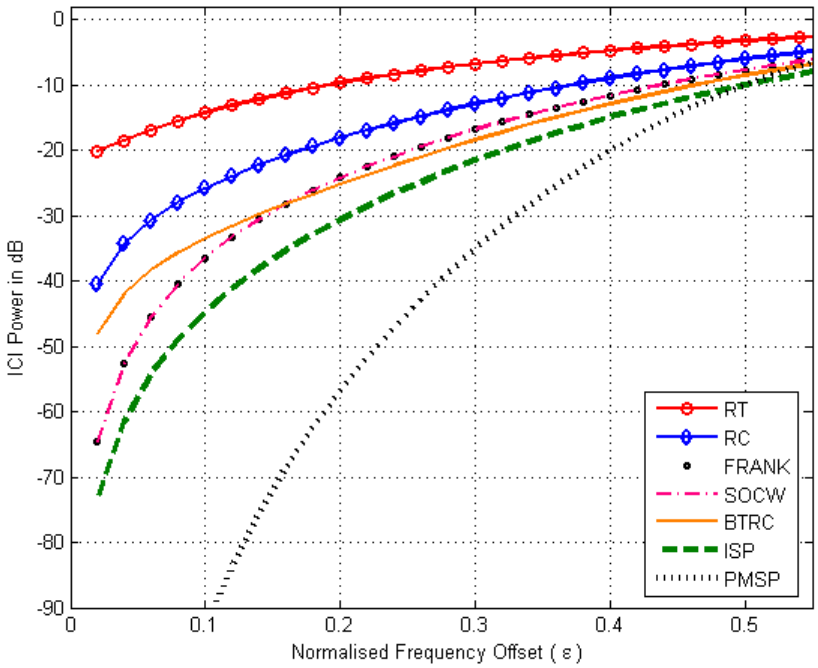

Figure-2.5.7: The average ICI power for 64 sub-carrier OFDM system with different window function at $\alpha = 1$

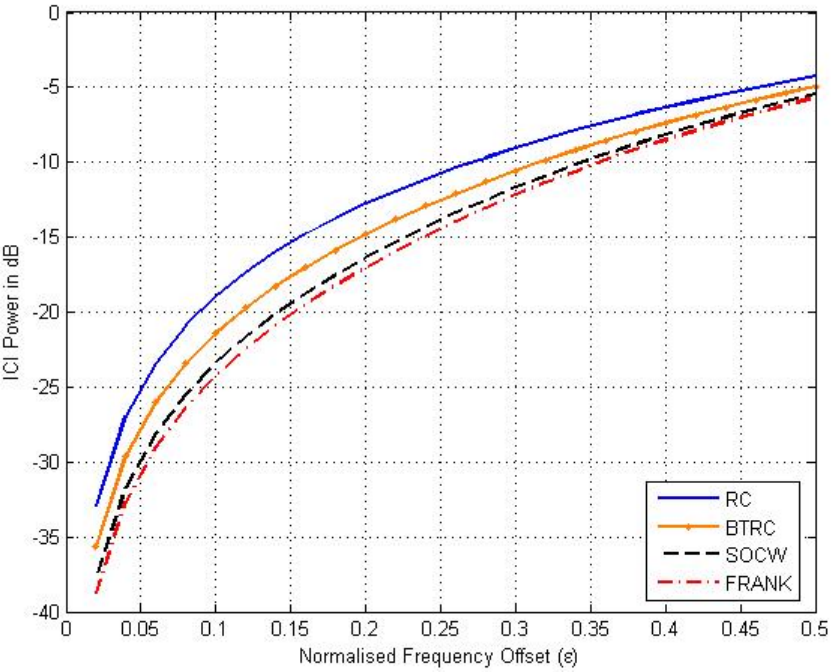

Figure-2.5.8: The average ICI power for 64 sub-carrier OFDM system with different window function at $\alpha = 0.5$

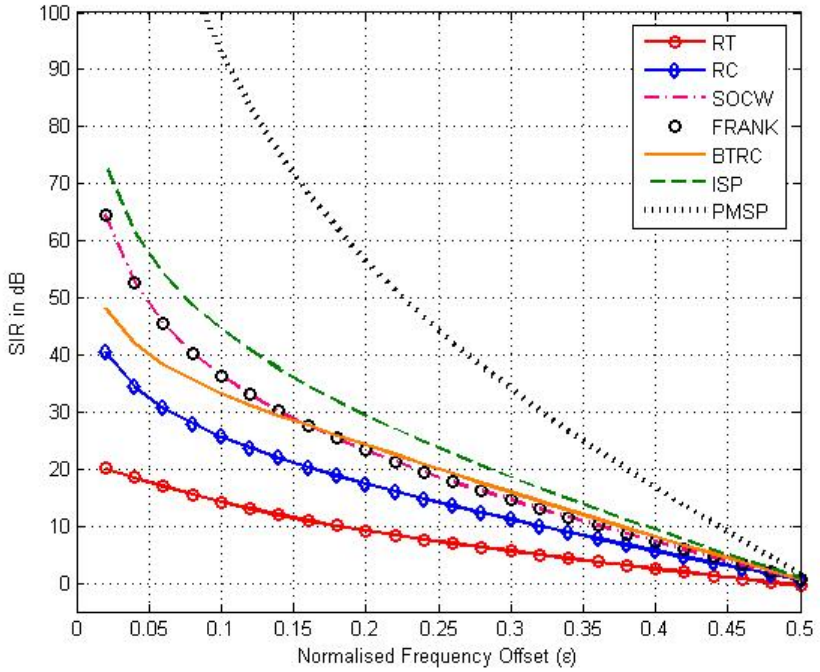

Figure-2.5.9: The average SIR for 64 sub-carrier OFDM system with different window function at $\alpha = 1$

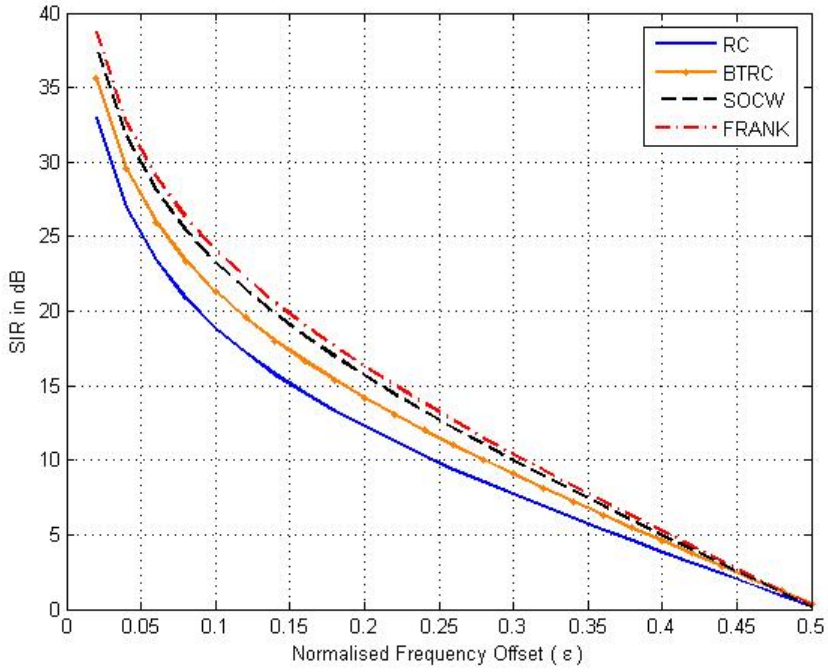

Figure-2.5.10: The average SIR for 64 sub-carrier OFDM system with different window function at $\alpha = 0.5$

2.5.2 ICI Self Cancellation Method.

The ICI self-cancellation is an efficient and simple method of ICI reduction. It has been suggested by Zhao *et.al* [**140**] in 1996, that the part of ICI can be canceled if the same symbol with different polarities is modulated on two adjacent sub-carriers and then transmitted. By using this method, the ICI depends on the difference between the adjacent weighting coefficients rather than on the coefficients themselves. As the difference between adjacent coefficients is small, the ICI will be less. If adjacent coefficients were equal, then the ICI would be completely cancelled.

This idea is again extended by Zhao *et.al* in 2001 [**141**] by modulating the same data in several adjacent sub-channels with optimal weights. The weighting coefficients are designed so that the ICI can be minimized. At the receiver side, by linearly combining the received signals on these subcarriers with proposed coefficients, the residual ICI contained in the received signals can then be further reduced. The SIR can be further improved if the group size is taken as two, three or more.

A general ICI self-cancellation method is also proposed by A. Seyedi *et.al* in 2005 [**12**]. This method uses windowing at the transmitter and receiver side for ICI self cancellation. The method proposed by Zhao et al can be considered as special case of this method. Although these methods can effectively mitigate ICI, the data transmission rate is also reduced since it is, in fact, repetitive frequency coding. A more advance self cancellation algorithm has been proposed by Ming-Xian Chang in 2007 [**84**]. This algorithm uses a pre-processor at transmitter and a post processor at receiver for ICI cancellation.

2.6 STATEMENT OF PROBLEM

The different issues of OFDM system have been reviewed in this chapter and the available results also verified with the simulation studies. The summary of this literature review is that besides so many advantageous features of OFDM system, there exist some problems which can affect the performance of OFDM system and if not properly handled then it may degrade the performance severely. Although, a lot of solutions of these problems or issues are available in the literature, but still there is a scope of providing better solution for each and every problem discussed above. Therefore, following problems are undertaken in this course of study-

I. Timing offset estimation

From the review of synchronization issue of OFDM system (section 2.4.1), it is clear that the correct timing offset is required at the receiver for finding the correct start of OFDM symbol. The performance of OFDM system may be degrades due to incorrect timing offset estimation. Therefore, it is required to apply an efficient timing offset estimator at the receiver.

Different solutions are available in the literature, but their performance degraded in frequency selective fading channel. Recently, the use of chirp signal as a training sequence gain popularity for synchronization purpose [**35, 71**]. It is also found after literature review, that the fractional Fourier transform (FRFT) is a better tool available for analyzing the signal when it is passed through time varying frequency selective fading channel **[7]**. After initial studies, it is found that FRFT based correlation theorem has never been used for timing offset estimation in OFDM system. Hence, an effort can be made to combine the use of FRFT and chirp signal for timing offset estimation.

II. Carrier frequency offset estimation

Carrier frequency offset is one of the major issues of OFDM system. CFO generates ICI which degrades the BER performance. Therefore, the CFO estimation is must required at the receiver before the recovery of information symbol. The estimator which gives minimum mean square error of estimation is the need of hour.

Several methods of CFO estimation are available in the literature, however, similarly as timing offset estimator their performance degrades in outdoor multipath channel. It is also found that chirp signal based CFO estimator performs better than other methods [**71**]. From literature survey, it has been found that the modulation property of FRFT is useful in determining the shift of frequency of signal. Therefore, an effort can be made to give an algorithm for CFO estimation using combination of chirp signal and FRFT.

III. High PAPR

The high PAPR of transmitted signal is another major problem of OFDM system. Due to this high PAPR, the efficiency of power amplifier is reduced and also orthogonality between sub-carriers lost which degrades the BER performance [**122**]. Different solutions of this problem are available in the literature and also discussed in section 2.3.2. But each has its own merits and demerits. Therefore, there is a scope of providing new PAPR reduction technique which provides better results in all terms.

As described in Section-2.3.2.5, that hybrid methods are better choice for PAPR reduction techniques. Clipping is the method which can be clubbed with any other method for PAPR reduction. Also, it is discussed that pre-coding or pulse shaping is simple and efficient method of PAPR reduction. The performance of Pre-coding method is depends on the pulse shaping function used [**75 and 105**]. Raised-cosine and square root raised cosine has been used in [**75**] and [**105**]. But still there are many pulse shapes which have been never used for pre-coding method.

Therefore, an attempt can be made in this direction (i.e. new pulse shape for pre-coding) and to combine pre-coding and clipping. Also, there is a scope of modifying conventional clipping process.

IV. ICI reduction using receiver windowing

The effect of all above mentioned problems are appearing in the form of inter-carrier interference (ICI) at the receiver. Several methods of ICI reduction are available in the literature [**25, 53, 54, 64, 84, 85, 86, 87, and 140**]. Out of which, receiver windowing gains so much popularity and attention due to its easy implementation and better performance. For receiver windowing, a Nyquist pulse shape with low side lobe level is required [**25, 86**]. Several pulse shapes are used for ICI reduction [**86**], but still there are some pulse shapes which are never used. So, there is a scope of using these pulse shapes for ICI reduction.

****